Local structure of As_xTe_{100-x} glasses studied by differential x-ray anomalous scattering and x-ray-absorption spectroscopy

Q. Ma
Laboratoire pour l'Utilisation du Rayonnement Electromagnétique, Bâtiment 209D, Université de Paris-Sud, 91405 Orsay Cedex, France

D. Raoux
Laboratoire de Cristallographie, Centre National de la Recherche Scientifique, 38042 Grenoble, France

S. Bénazeth
Laboratoire de Chimie Minérale, Faculté de Pharmacie, Chatenay-Malabry, Université Paris XI, France and Laboratoire pour l'Utilisation du Rayonnement Electromagnétique, Bâtiment 209D, Université de Paris-Sud, 91405 Orsay Cedex, France

(Received 19 March 1993)

The local structure of As_xTe_{100-x} glassy semiconductors has been studied using x-ray anomalous scattering and x-ray-absorption spectroscopy as a function of the composition. Two important findings are (a) tellurium (Te) atoms are twofold coordinated in arsenic (As) rich alloys ($x > 40$), while the Te coordination suddenly increases to 2.4 at the stoichiometric $As_{40}Te_{60}$ composition, which indicates a large fraction (about 50%) of threefold Te sites in this glass. This percentage of occupancy of the threefold Te sites remains almost constant with increasing further the Te concentration; (b) a significant level of chemical disorder, marked by the existence of homopolar As-As and Te-Te pairs in the first coordination shell, is observed for all the investigated glasses. At the $As_{40}Te_{60}$ composition, nearly about the same amount of As-As and Te-Te pairs do exist in the first coordination shell. Thus the stoichiometric $As_{40}Te_{60}$ composition is not a chemical threshold as it is the case for the Se- or S-based glasses. Based on these results, a number of peculiar and unique features in the physical properties of these glasses, such as the glass transition temperature (T_g), the microhardness, the glass forming ability, and the electrical conductivity, can be understood.

I. INTRODUCTION

The ultimate goal for the structural study of amorphous materials is to try to understand their macroscopic properties in terms of their microscopic structure. In recent years, chalcogenide glasses have created a great deal of interest due to their semiconducting properties. In comparison with the sulfur and selenium-based glasses, which have been extensively studied,[1] the tellurium-based glasses have been far less investigated. This is especially true for the As_xTe_{100-x} glasses. Among chalocogenide glasses, the As_xTe_{100-x} glasses have the highest electric conductivities[2] and present switching and memory properties[3] as well as a deep transmission in the infrared band of the electromagnetic spectrum.[4] A systematic study of these glasses carried out by Cornet and Rossier[5] shows a number of peculiar and unique features in their physical properties. For instance, the glass forming ability (GFA) is maximal at the eutectic $As_{46}Te_{54}$ and $As_{27}Te_{73}$ compositions, but minimal at the stoichiometric $As_{40}Te_{60}$ composition while, on the contrary, the GFA for As_xS_{100-x} or As_xSe_{100-x} systems is maximal at the stoichiometric composition. The T_g monotonically increases with the As content while for As_xS_{100-x} or As_xSe_{100-x} glasses, it shows a maximum at the stoichiometric composition.

In an early x-ray-diffraction study[6] of the $As_{40}Te_{60}$ glass, it was already claimed that the glassy structure is a random packing of $AsTe_{3/2}$ pyramidal units and that the local coordination in the glass is different from that in the crystalline phase. Cornet and Rossier[7] also carried out the structural study using mainly an x-ray-diffraction technique for the As_xTe_{100-x} glasses with $x = 30-60$. Their main achievements are summarized as follows.

(a) At the $As_{40}Te_{60}$ composition, arsenic atoms are threefold coordinated by tellurium ones and Te atoms are twofold coordinated by As ones with full chemical ordering, as reported in Ref. 6.

(b) For As-rich glasses ($x > 40$), an additional As site emerges as x increases, which has one As and two Te neighbors. The short strong covalent As-As bond is considered as a pair lock stabilizing the glassy structure.

(c) For Te-rich glasses ($x < 40$), As atoms are still threefold coordinated while Te atoms are twofold and threefold coordinated and the concentration of the threefold Te sites rapidly increases with the increase of the Te content. By using x-ray photoemission spectroscopy (XPS) and neutron scattering,[8] they also suggested the existence of the sixfold As sites in Te-rich glasses. The ex-

istence of threefold Te sites has also been indicated by Tenhover, Boolchand, and Bresser[9] using Mössbauer spectroscopy.

Later, an extended x-ray-absorption fine-structure (EXAFS) at the As K edge was performed for the $As_{40}Te_{60}$ glass by Pettifer[10] using synchrotron radiation. He pointed out that a minimum at about 130 eV in the spectrum might be either due to a splitting of the first Te shell or to a minimum in the Te backscattering amplitude. A theoretical simulation performed by using the curved wave approximation gave the best fit of the data when assuming two Te atoms at 2.67 Å and one As atom at 2.52 Å. Thus he suggested the necessity of including homopolar As-As bonds to account for the strong minimum at 130 eV.

Obviously the structural information concerning the local chemical order in the $As_{40}Te_{60}$ glass is controversial. Moreover, both the increase of the mean coordination number of the Te atoms and the existence of sixfold As sites, suggested for Te-rich glasses, lack experimental evidence. The higher glass forming ability at the eutectic composition ($x=27$) was explained by Cornet and Rossier as resulting from an equilibrium of competition between twofold and threefold Te sites. Such an interpretation is somewhat too crude and does not provide a picture of the involved mechanism. It also lacks experimental support. Phillips has discussed[11] the use of the constraint theory to explain the GFA of covalent glasses. This theory is rather successful for the sulfur- and selenium-based chalcogenide glasses such as Ge_xSe_{100-x}, As_xS_{100-x}, and As_xSe_{100-x}. For these glasses, the maximum of the GFA is correctly predicted to occur at the so-called percolation threshold, where the mean coordination number is 2.4. Based on the available structural information, the maximum of the GFA for the As_xTe_{100-x} glasses should also occur at the stoichiometric $As_{40}Te_{60}$ composition since the mean coordination number for this composition is equal to 2.4 as well. This is inconsistent with the experimental observation of a minimum in the GFA. In fact, our present knowledge lacks a detailed and accurate description of the glassy As_xTe_{100-x} structures and does not allow a comprehensive understanding of the unique features in the physical properties of the glasses.

The reason for the limited structural information yielded by the previous studies lies in the lack of suitable techniques for the structural investigations, e.g., the lack of suitable isotopes to use neutron diffraction to separate out the partial distribution functions. That is why we have undertaken a structural study of these glasses by using x-ray-absorption spectroscopy and x-ray difference anomalous scattering (DAS), which are relatively new. Both of them can provide selective structural information. A DAS spectrum can be analyzed down to $k=0$. This yields information about the structure over the medium range up to 8 or 10 Å. In this respect, the DAS technique is complementary to EXAFS, for which the low k part, e.g., below ~ 3.5 Å, of an EXAFS spectrum has to be cut since it is difficult to interpret due to the multiple-scattering processes. The medium range structure derived from a determination of partial structure factors based on the data from our anomalous scattering measurements will be discussed in another paper. In this paper, we report the results about the local structure and discuss its relation with some physical properties of the glasses. In Sec. II, we describe the sample preparation, the experimental procedure and the data processing. We give the results from our EXAFS analysis in Sec. III and a description of our DAS results in Sec. IV. In Sec. V, we try to explain some peculiar features in the physical properties of the glasses, such as the GFA, the Tg, the microhardness, and the transport property, in terms of the microscopic structure.

II. EXPERIMENTAL AND DATA PROCESSING

A. Sample preparation and characterization

The formation of homogeneous As_xTe_{100-x} glassy materials by quenching the liquid state has been observed over a large range of compositions, for $40<x<60$ by Tsugane, Haradome, and Hioki,[12] $20<x<70$ by Cornet and Rossier,[13] $40<x<75$ by Quinn,[14] $43<x<70$ by Tenhover, Boolchand, and Bresser,[15] and $45<x<65$ by Savage.[16] Our sample preparation method is based on the procedure described by Rouland *et al.*[17] We have prepared five glassy samples with arsenic concentration $x=20$, 30, 40, 50, and 60. Except for $x=40$, they have been obtained in the following way: chemically pure As and Te (99.999%) are weighted according to the desired composition. Their mixture is immediately sealed in an air evacuated silica ampoule (external diameter 6 mm, length 30 mm), which is then heated in an electric oven. The temperature is slowly raised up to 200 °C above the melting point and the melt is kept at this temperature, typically for 24 h. Then quenching the melt into water yields the glassy state material. A 0.2–0.5 g sample can be obtained at each preparation, depending on the composition. However, the glassy state at the stoichiometric $As_{40}Te_{60}$ composition cannot be prepared by a water quench. Glassy ribbons have thus been obtained by using the melt spinning method,[18] which provides a quenching rate higher than 10^5 °C/sec. We have characterized our samples by x-ray large- and small-angle scattering and by EXAFS and electron microscopy as well.

(a) All the samples have been checked to be amorphous by x-ray diffraction. The EXAFS spectra measured for the glasses are very different from those for the crystalline $As_{40}Te_{60}$ phase, as will be shown in the following section. The EXAFS oscillations for the crystal are much weaker than for the glasses. Since EXAFS takes place only over a length of a few angstroms, the difference in the spectra should be due to the difference in the local structures. Thus it rules out the possibility that the glasses are aggregates of microscystalline grains.

(b) To check the possible existence of segregations, x-ray small-angle scattering measurements have been performed for the $As_{50}Te_{50}$ and $As_{40}Te_{60}$ glasses. There are no scattering patterns in the range from 0.1 to 0.8 $Å^{-1}$ for both samples. This indicates a homogeneous structure over distances of about 60 Å at least. Electron microscopy preliminary results for the $As_{40}Te_{60}$ glass sug-

gest that there is no phase segregation over larger distances in the bulk of grains, except maybe on their surface.[19]

The crystalline $As_{40}Te_{60}$ β phase was prepared following the procedure described in Ref. 20 and used as a reference material for heteropolar As-Te or Te-As pairs in the EXAFS analysis. The homogeneity and purity of the $As_{40}Te_{60}$ β phase have been checked by x-ray diffraction. Moreover, amorphous As and metallic Te were used as reference materials for homopolar As-As and Te-Te pairs. In the β phase, As atoms are sixfold coordinated by Te ones with three neighbors at 2.735 Å and with three other ones at a larger distance of 3.15 Å. Te atoms occupy two different sites. Two thirds of them are coordinated by three As atoms at 2.735 Å and further by three Te neighbors at a larger distance of 3.68 Å, and one third by six As atoms at 3.15 Å. In average, each Te atom is thus coordinated by four As neighbors (two at 2.735 Å and two at 3.15 Å). In fact, the crystalline structure can be considered as a stacking of five atomic planes (TeAsTeAsTe), coupled together by weak Van der Waals forces. The structure of amorphous As is based on pyramid-shaped four-atom molecular units in which As is threefold coordinated at 2.47 Å.[21] The structure of elemental Te is isomorphous to that of Se, which is aggregates of zigzag chains, Te atoms being twofold coordinated with an interatomic distance of 2.86 Å.[22]

B. EXAFS experiment and data processing

EXAFS measurements were performed at the As K edge (11 867 eV) in transmission mode at the EXAFS IV station, using the beam delivered from a bending magnet at DCI in LURE. Experiments at the Te K edge (31 830 eV) were performed at the Romeo II EXAFS station at HASYLAB (Hamburg). Unfocussed Si (311) monochromators were used in both cases. Data were taken at room and liquid-nitrogen temperatures with an energy step of 2 eV using ionization chambers as detectors for both edge measurements, data at the absorption edges being collected with a 0.5 eV step.

We have measured the x-ray absorption spectra for the reference materials and for the As_xTe_{100-x} glasses. The samples were prepared by crushing and grinding the materials into particles finer than 20 μm, which are then homogeneously stacked on Kapton tapes. The number of tapes used for the measurement varies with composition, the criterion being to get a jump of about 1 at the absorption edge. Several samples of different thicknesses were measured to make sure than the EXAFS amplitudes were not reduced by pinhole effects.

The EXAFS oscillations $X(k)$ were separated from their backgrounds by using Victoreen fits. The electron wave vector k is defined as $[2m(E-E_0)/\hbar^2]^{1/2}$, where E and E_0 are, respectively, the energy of the measurement and that of the absorption threshold. By making a number of approximations,[23] like the single scattering and plane-wave ones, $X(k)$ is given by

$$\chi(k)=\frac{m}{4\pi^2\hbar^2 k}\sum_j \frac{N_j F_j(2k)}{r_j^2} e^{-2r_j/\lambda} e^{-2\sigma_j^2 k^2} \times \sin[2kr_j+\psi_j(k)] \,. \quad (1)$$

$F_j(2k)$ is the backscattering amplitude scattered by each of the N_j neighboring atoms of the jth type located at a distance r_j from the photoexcited (absorbing) atom and $\psi_j(k)$ is the total phase shift experienced by the photoelectron, being equal to $\phi_a(k)+\phi_j(k)$, where $\phi_a(k)$ and $\phi_j(k)$ are, respectively, the phase shifts due to the absorbing and scattering atoms (the absorbers and scatterers). Both $F_j(2k)$ and $\psi_j(k)$ are chemically sensitive. σ_j is the Debye-Waller factor which is the standard deviation of interatomic distances relative to their mean value r_j. The damping term $e^{-2r_j/\lambda}$ is due to inelastic losses in the scattering process, $\lambda(k)$ being the electron mean free path which is taken as k/Γ in our case. The Γ value is obtained from the calibration of the EXAFS spectra of the reference materials. In Eq. (1), we neglect intratomic effects within the absorbing atom which are in fact incorporated in the backscattering amplitude. Through the EXAFS analysis, the information about N_j, r_j, and σ_j around the absorbing atom can, in principle, be obtained for each partial coordination shell. The modulus of the sine Fourier transform (FT) of Eq. (1) gives a pseudoradial distribution function (RDF) in real space.

Figure 1 shows the EXAFS spectra measured at room

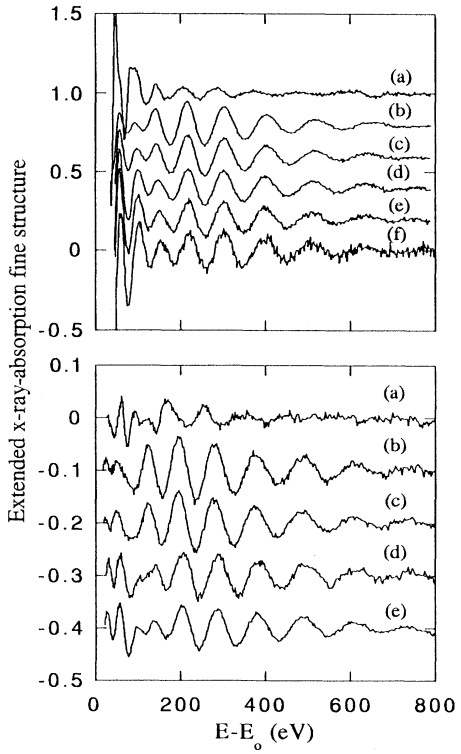

FIG. 1. Compositional dependence of the glassy EXAFS spectra measured at room temperature around the As (above) and Te (below) K edges: (a) β-$As_{40}Te_{60}$ crystal, and the glasses (b) $As_{60}Te_{40}$, (c) $As_{50}Te_{50}$, (d) $As_{40}Te_{60}$, (e) $As_{30}Te_{70}$, and (f) $As_{20}Te_{80}$.

temperature at the As and Te K edges for the $As_{40}Te_{60}$ crystal and for the glassy samples. As already mentioned earlier, the EXAFS oscillations are much weaker for the $As_{40}Te_{60}$ crystal than for the glasses. This is not the usual case. Similar observations were obtained for measurements at liquid-nitrogen temperature (LNT). Figure 2 displays the moduli of the Fourier transforms of the k^3 weighted EXAFS spectra of the crystalline and glassy $As_{40}Te_{60}$ phases measured at LNT. The FT moduli for the glassy phase are much more intense than those for the crystalline phase.

In order to analyze the glassy EXAFS spectra, we need an accurate knowledge of the phase shifts and amplitudes for the heteropolar As-Te or Te-As ones. Obviously, the amplitudes extracted from the cystalline β-$As_{40}Te_{60}$ spectra cannot be directly used because they are too weak. We point out that trials to get a better reference have not been successful since the EXAFS spectra of crystalline telluride compounds which involve atoms close to As, like GeTe, for instance, also exhibit weak oscillations. We thus considered the use of amplitudes and phase shifts calculated by Mac Kale *et al.*[24] These data should be reasonably accurate in the low k range since being calculated in the curved wave approximation at several interatomic distances. We have thus interpolated Mac Kale *et al.*'s data at the specific distance of interest. In order to determine the Γ value, we have tried to fit the EXAFS spectra of the reference materials using Mac Kale *et al.*'s data and the crystallographic data N_j given in Sec. II A. This also allows us to determine the best value of the threshold energy E_0 used to calculate the momentum k.

A good quality of simulations is achieved for all the references, as shown in Fig. 3, and the parameters determined from these calibrations are given in Table I. We point out that, for the AsK edge, the interatomic As-As and As-Te distances determined from the fits agree with their crystallographic values within $\sim$0.01 Å and that there is a reasonable energy shift ΔE_0 with respect to the threshold energy. For the Te K edge, the interatomic Te-Te and Te-As distances determined from the fits are shorter by 0.04 Å than their crystallographic ones and a large energy shift (~ -12 or -25 eV) is needed. This suggests a poorer quality of Mac Kale *et al.*'s phase shifts for heavy atoms like Te. We also notice that the

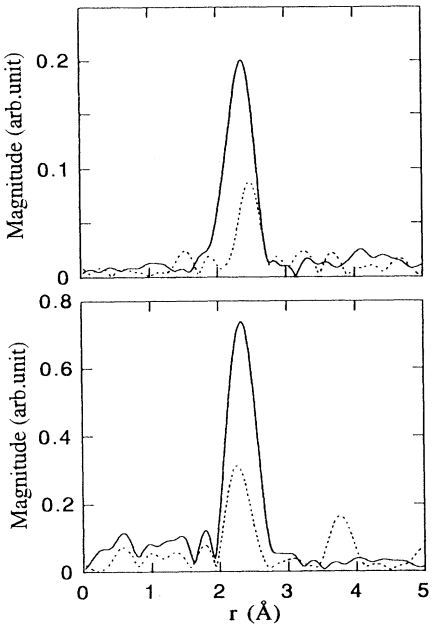

FIG. 2. The moduli of the k^3 weighted Fourier transforms of the As (above) and Te (below) K edges EXAFS spectra (LNT) of glassy (full line) and crystalline (dashed line) $As_{40}Te_{60}$ states. They were calculated by using the data from $k=3.5$ to ~ 14 $Å^{-1}$.

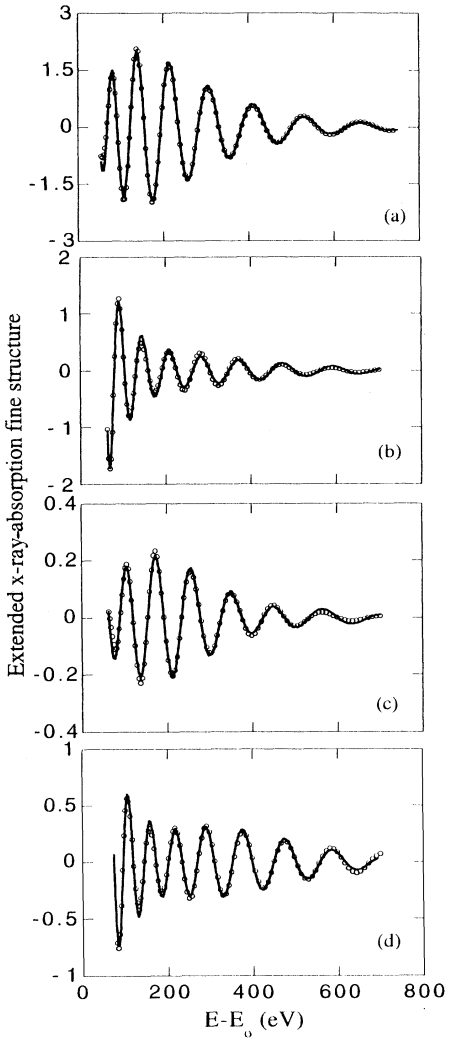

FIG. 3. Simulations of the reference EXAFS spectra by using Mac Kale *et al.*'s amplitudes and phase shifts with only the coordination numbers fixed: (a) amorphous As, (b) β-$As_{40}Te_{60}$ crystal at the As K edge, (c) β-$As_{40}Te_{60}$ crystal at the Te K edge, and (d) metallic Te. Fits are shown by dots and the experimental data by full lines.

TABLE I. The r, Γ, σ, and ΔE_0 values yielded from the fitting of the reference EXAFS spectra using Mac Kale's data. Crystallographic values are given in parentheses.

	Amorphous As	Metallic Te	Crystalline $As_{40}Te_{60}$	
	As K edge	Te K edge	As K edge	Te K edge
r (Å)	2.475 (2.47)	2.82 (2.86)	2.724 (2.735)	2.693 (2.735)
σ (Å)	0.083	0.076	0.102	0.100
Γ (Å^{-2})	1.00	2.98	2.00	3.98
ΔE_0 (eV)	~8.9	~−12.0	~2.8	~−25.0

contribution from the shells at 3.15 Å in the β-$As_{40}Te_{60}$ crystal is negligible for both the As- and Te-edge EXAFS, which are thus dominated by the contribution of the scatterers at 2.735 Å. It is noteworthy that the values of the Debye-Waller factors σ are the same for the As-Te and Te-As pairs, determined, respectively, from the fits of the As and Te K edge EXAFS spectra of β-$As_{40}Te_{60}$. This demonstrates the coherency of the analysis and indicates that the quality of the calculated amplitudes is rather good. However, the accuracy of Mac Kale *et al.*'s amplitudes may not be precisely checked at large k (or E) values for the heteropolar pairs because of the strong damping of the β-$As_{40}Te_{60}$ EXAFS oscillations. This is one of the reasons for which we also used the x-ray anomalous scattering method to check on a few cases the validity of our EXAFS results.

C. Anomalous scattering experiment and data processing

The differential anomalous x-ray scattering (DAS) technique makes use of the resonant changes in the x-ray scattering factor ($f=f_0-f'+if''$) of an atom when the x-ray energy is tuned close to its absorption edge.[25] It provides another possibility to probe selectively the ordering around each component in amorphous materials, though it is less chemically sensitive than EXAFS because it lacks the phase information. Its use, however, does not rely on the availability of reference materials as much as EXAFS does. This is an advantage over EXAFS. Thus, for the As_xTe_{100-x} glasses, it may allow us to avoid the difficulty met in the calibration of the amplitudes for the As-Te and Te-As pairs. Safer information may be obtained in particular about the mean coordination number around each component in the glass. We have thus measured the scattering from three glassy samples with arsenic concentration $x=20$, 40, and 50, which have already been investigated by EXAFS.

The x-ray scattering experiments at wavelengths around the As and Te K edges were carried out using a two axis vertical diffractometer in the symmetric reflection mode using the x-ray beams delivered from a bending magnet and a superconducting wiggler, respectively, at DCI in LURE. Unfocused double crystal [Si(220)] monochromators were employed in both cases to select the beam energy. The intensities scattered by the three samples were registered using a Si:Li solid-state detector with an energy resolution of about 200 eV at 12 000 eV.

For an alloy, the x-ray scattered intensity I is connected to the structure factor $S(q,E)$ through

$$I=N[\langle f(q,E)^2\rangle+\langle f(q,E)\rangle^2(S(q,E)-1)]\ , \qquad (2)$$

where N is the number of atoms in the sample, $\langle\ \rangle$ means the chemical average, $q=4\pi\sin\theta/\lambda$ is the magnitude of the scattering vector (note that $2k$ in EXAFS is the scattering vector equivalent to q in x-ray scattering), and for a binary alloy,

$$S(q,E)=\sum_{i,j} W_{ij}(q,E)S_{ij}(q)\quad (i,j=A\ \text{or}\ B)$$

in which $S_{ij}(q)$ is the partial structure factor (PSF) and

$$W_{ij}(q,E)=\frac{c_ic_jf_i(q,E)f_j(q,E)}{\langle f(q,E)\rangle^2}\ ,$$

where c_i or c_j is the atomic fraction for atoms of the species i or j. If two measurements are performed at two different x-ray photon energies in the vicinity of the absorption edge of one atomic species, for instance, of atom A, the difference of the two scattering patterns can be expressed as

$$\Delta I=\Delta_A[\langle f(q,E)^2\rangle-\langle f(q,E)\rangle^2]+\Delta_A\langle f(q,E)^2\rangle S_A^{\text{diff}}(q)\ , \qquad (3)$$

where $S_A^{\text{diff}}(q)$ is a difference structure factor (DSF) containing only the PSFs which involve atom A. The information about B-B correlation pairs is eliminated since the atomic scattering factor of atom B does not vary appreciably with the x-ray wavelength in the vicinity of the absorption edge of atom A. Similarly, $S_B^{\text{diff}}(q)$ can be obtained if the measurements are performed around the absorption edge of atom B. As the RDF is defined as the sine Fourier transform of $q[S(q,E)-1]$, we can equally define a difference distribution function (DDF) as

$$\text{DDF}_i(r)=4\pi r^2\rho_0+\frac{2r}{\pi}\int q[S_i^{\text{diff}}(q)-1]\sin(qr)dq \quad (i=A\ \text{or}\ B)\ . \qquad (4)$$

The $\text{DDF}_i(r)$ is a chemically specified RDF which contains the contributions from only the A-A and A-B (or A-B and B-B) correlation pairs and thus provides a selective structural information as EXAFS does. The area of a peak in the $\text{DDF}_i(r)$ yields an average coordination number around atoms and by an hypothetical scatterer with a scattering factor equal to the average value $\langle f\rangle$. It is, in fact, a linear combination of the two partial coordination numbers times, respectively, their weights (P_{ij}),

which are the Fourier transforms of $W_{ij}(q,E)$'s.

In our data processing, the energy independent part (f_0) of the atomic scattering factor is taken from tabulated values.[26] The f' and f'' values far from the edges (11 103 and 30 215 eV) are taken from Sasaki's data[27] which are calculated for free atoms. The f'' values around both edges (11 864 and 31 793 eV) were determined from the EXAFS measurement while the f' values were calculated by using the Kramers-Kronig relationship. In the calculation, the near-edge range f'' values from EXAFS are matched to Sasaki's theoretical data to meet the requirement of a large integration range.[28] The values of the measuring energies and of the corresponding f' and f'' for the $As_{40}Te_{60}$ glass are given in Table II. Note that the relative change $\Delta f/f$ is about 0.3 for the arsenic atom, while it is only about 0.1 for the tellurium atom.

Since a Si:Li solid detector is used to register the data, the elastic and inelastic scattering intensities cannot be resolved. When using x-ray wavelengths close to an absorption edge, the K_β fluorescence or Raman resonant scattering which is excited can neither be separated. The intensity of the inelastic Compton scattering is simulated by using the formula given by Palinkas.[29] The subtraction of the K_β fluorescence from the intensity registered at wavelengths near the edge is performed by scaling the intensity of the K_α fluorescence by a ratio K_β/K_α. The measurement of this ratio is performed at an energy high enough above the absorption edge so that the scattering and the K_β fluorescence are separated by the detector. The value of the ratio has been corrected for absorption. For the As fluorescence, the value is found to be 0.17 and for the Te one 0.19. Since the center of the synchrotron radiation beam is extremely well horizontally polarized and since we use a vertical diffractometer, the polarization correction is weak. The scattered intensity is normalized by the K_α fluorescence one in order to eliminate possible geometrical effects like the distortion at small angles due to the limited sample size, since both processes follow the same optical path. Finally, the normalization constant, which is necessary to get the intensity per atom, is determined by the Krogh-Moe and Norman[30] integral method.

The structure factors derived from the intensities registered at several x-ray wavelengths for the $As_{50}Te_{50}$ glass are shown in Fig. 4 as an example. They show only a weak energy dependence. This is the reason why the DSFs are rather noisy, as shown in Figs. 5 and 6 for the $As_{50}Te_{50}$ and $As_{40}Te_{60}$ glasses. We point out that a prepeak appears at about 1 Å in the As-edge DSF of the $As_{50}Te_{50}$ glass as well as in that of the $As_{40}Te_{60}$ one, which is not found either in the Te-edge DSFs or in the

TABLE II. f' and f'' values for the $As_{40}Te_{60}$ glass.

Energy (eV)	f'_{As}	f''_{As}	f'_{Te}	f''_{Te}
11 103	−2.4	0.56	−0.2	3.70
11 864	−9.2	1.01	−0.3	3.30
30 215	0.14	0.76	−2.0	0.60
31 793	0.13	0.69	−6.5	0.65

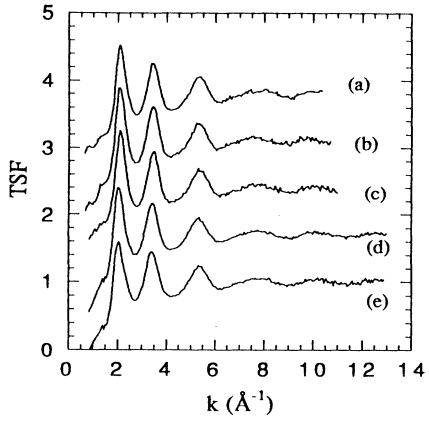

FIG. 4. The structure factors measured at different x-ray energies for the $As_{50}Te_{50}$ glass. (a) 11 103, eV, (b) 11 864 eV, (c) 12 658 eV, (d) 30 215 eV, (e) 31 793 eV.

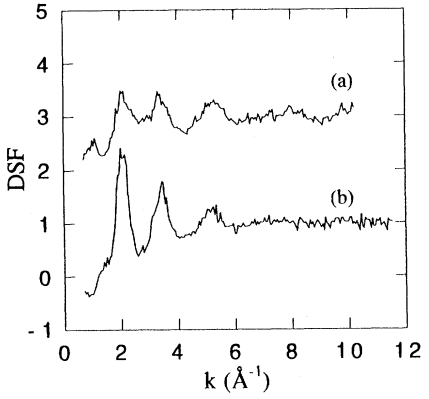

FIG. 5. The difference structure factors (DSF) of the $As_{50}Te_{50}$ glass obtained around the (a) As and (b) Te K edges.

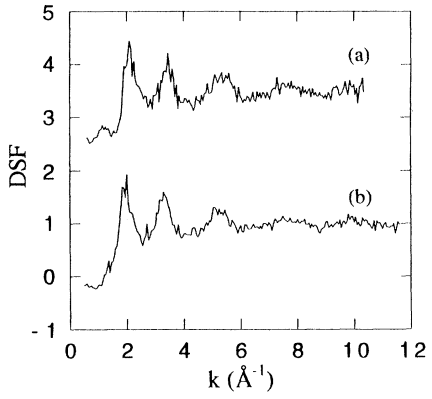

FIG. 6. The difference structure factors (DSF) of the $As_{40}Te_{60}$ glass obtained around the (a) As and (b) Te K edges.

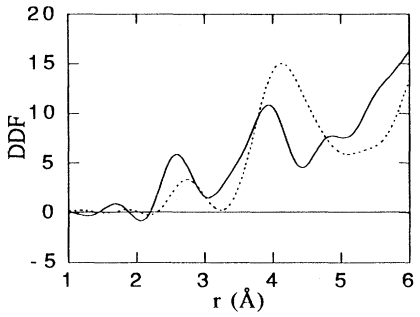

FIG 7. The difference radial distribution functions (DDF) for the $As_{50}Te_{50}$ glass obtained around the As (full line) and Te (dashed line) K edges.

total structure factors. It is thus due to cation-cation correlations (As-As ones) extending over distances up to 8 $Å^{-1}$, as is also the case for Ge-Se glasses.[25,31] Due to the weak As concentration, we could not get a correct DSF around the As edge for the $As_{20}Te_{80}$ glass. Also due to the low As concentration and to the strong decrease of f_{As}, the measurement performed near the As edge contains contribution from the As-As pairs as weak as 1.2%. It yields a structure factor, which is, in fact, equivalent to a Te-edge DSF. Thus the DAS measurement around the Te K edge is not necessary for the $As_{20}Te_{80}$ glass. The Fourier transforms of these DSFs are performed using the data up to about 9.5 $Å^{-1}$ and the corresponding DDFs are shown in Figs. 7 and 8.

III. EXAFS RESULTS

We first discuss some qualitative findings. From Fig. 1 we notice that beat nodes appear at low energies in all the glassy spectra and that they evolve with composition. The FTs of these spectra are shown in Fig. 9. There is no information on higher shells in any case. Thus the beat node should result from the interference of the backscattering from scatterers at different distances in the first shell. We also note that the position of the maximum shifts towards a higher distance with the increase of the Te content. In the case of the As K edge, a shoulder appears for the Te-rich glasses on the lower distance side of the pseudo RDFs and its magnitude enhances with the Te constant. It is characteristic of the Te backscattering since a similar shoulder also appears in the FT of the elemental Te EXAFS spectrum. The increase in its intensity as well as the shift of the peak position evidence an increase in the number of Te scatterers with the increase of the Te concentration, and thus suggest the existence of As scatterers in the first shell for As-rich glasses which tend to smear out the shoulder.

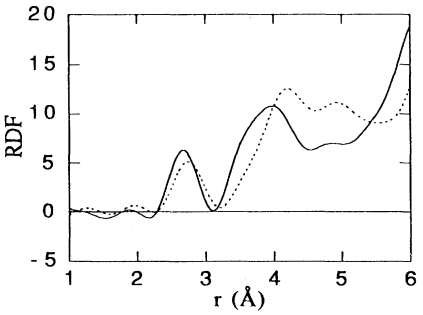

FIG. 8. The difference radial distribution functions (DDF) for the $As_{40}Te_{60}$ glass obtained around the As (full line) and Te (dashed line) K edges.

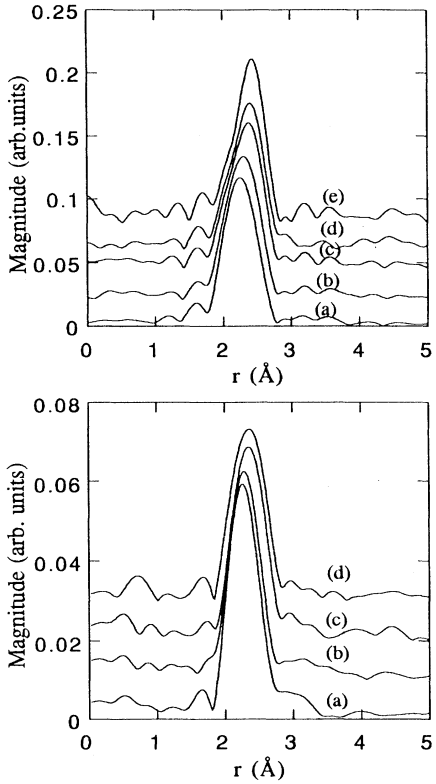

FIG. 9. The moduli of the k^3 weighted Fourier transforms of the glassy EXAFS spectra around the As (above) and Te (below) K edges: the glasses (a) $As_{60}Te_{40}$, (b) $As_{50}Te_{50}$, (c) $As_{40}Te_{60}$, (d) $As_{30}Te_{70}$, and (e) $As_{20}Te_{80}$. Fourier transforms were performed by using the data from $k=3.5$ to ~ 14 $Å^{-1}$.

For the $As_{40}Te_{60}$ composition, Fig. 2 compares the FTs of the glassy and crystalline EXAFS spectra. It is to be noted that the pseudo radial distance in the case of the Te edge is larger for the glass than that for the crystal, while it is shorter in the case of the As edge. This suggests that for the glass, the peaks are not only due to As-Te correlations as is the case for the crystalline phase. Homopolar As-As or/and Te-Te bonds have to occur. Thus a chemical disorder exists in the first shell in this glass. Figure 10 specifically compares the filtered As-edge EXAFS spectra for the $As_{40}Te_{60}$ (full line) and $As_{20}Te_{80}$ (dashed line) glasses. The difference is weak beyond 200 eV, but large below that energy. Since the $As_{20}Te_{80}$ glass is very rich in the Te content, As atoms are expected to be mainly binded to Te ones. In that case, the EXAFS amplitude

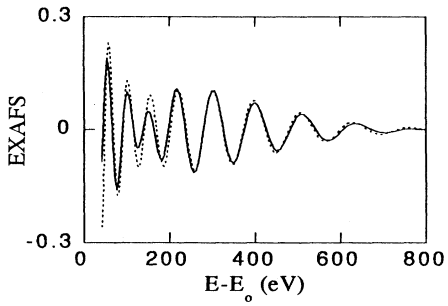

FIG. 10. Comparison of the filtered EXAFS spectra of the first coordination shells for the $As_{40}Te_{60}$ (full line) and $As_{20}Te_{80}$ (dashed line) glasses.

should essentially be due to the backscattering from Te scatterers. Thus, the difference between the two spectra observed at low energies in Fig. 10 suggests that the EXAFS spectrum of the $As_{40}Te_{60}$ glass contains not only the contribution from the Te neighbors but also that from other chemically different ones whose amplitudes peak up in the energy range from 100 to 200 eV. This is the case for the As scatterer. Thus homopolar As-As pairs do exist in the first shell in the $As_{40}Te_{60}$ glass.

We also find that the evolution of the Te-edge EXAFS spectra in the energy range below 200 eV (Fig. 1) may suggest that the Te local environment in the $As_{40}Te_{60}$ glass is rather similar to that in the $As_{30}Te_{70}$ glass, which is rich in Te, while being rather different from those in As-rich glasses. This similarity suggest the possible existence of Te-Te bonds in the $As_{40}Te_{60}$ glass. In summary, the qualitative findings mentioned above suggest a splitting of the first coordination shells around both As and Te atoms into two subshells, probably chemically different, for almost all the investigated glasses, surely including the $As_{40}Te_{60}$ one.

These findings are quantitatively supported by the attempts to fit the EXAFS data. By using Mac Kale *et al.*'s phase shifts and amplitudes, we failed to reconstruct the glassy spectra with the assumption of only heteropolar pairs occurring at one or even two distances. We thus had to assume the occurrence of homopolar As-As and Te-Te bonds, that is, for the As K edge we assumed the existence of As-As and As-Te bonds and for the Te K edge that of Te-As and Te-Te bonds. During the fitting procedure, the Γ values were kept fixed at the values given in Table I for each kind of atomic pair, but the structural parameters N_j, r_j, and σ_j as well as the energy threshold E_0 were allowed to float. For the values given in Table III, a good quality of fit is obtained for all the glasses, even in the energy range where a beat node occurs. Typical examples are shown in Fig. 11. We have found that the Te-As distance determined for the glasses from the Te-edge fit is shorter by ~ 0.03 Å than the As-Te one determined from the As-edge fit. This suggests that the distance determinations suffer from the same effects as the ones found in the case of the reference samples, i.e., Mac Kale *et al.*'s phase shift $\phi_a(k)$, when the Te atom is the absorber, was shown to yield short distances (by 0.04 Å). Moreover, in each case, an energy shift similar to the one used to fit the EXAFS data for the references was also required. Thus we accordingly corrected the distance values determined from the Te-edge analysis as well as the As-Te distance from the As-edge analysis by the differences shown in Table I (respectively, 0.04 and 0.01 Å). Our simulations clearly show that the beat nodes in the spectra do result from the interference of the two EXAFS signals produced by two chemically different types of atomic pairs at different interatomic distances. From Table III, we find that for the As-Te pairs, the Debye-Waller factors, and the interatomic distances determined using the As and the Te K edge EXAFS data are equal within 10% and 0.01 Å, respectively, and that the chemical compliance such that

$$N_{\mathrm{AsTe}} = (c_{\mathrm{Te}}/c_{\mathrm{As}})N_{\mathrm{TeAs}}$$

is observed. These demonstrate the coherency within our results. Moreover, the coordination number around the As atom is roughly equal to 3 for whatever the composition, which is a reasonable coordination number for As in amorphous materials.

In order to evaluate the error bars for the coordination

TABLE III. Structural parameters for the As_xTe_{100-x} glasses.

As K edge		As-As			As-Te		N_{As}
Sample	N	r (Å)	σ (Å)	N	r (Å)	σ (Å)	
$As_{60}Te_{40}$	2.1	2.47	0.060	1.0	2.67	0.060	3.1
$As_{50}Te_{50}$	1.6	2.47	0.060	1.4	2.66	0.064	3.0
$As_{40}Te_{60}$	0.8	2.47	0.050	2.2	2.66	0.064	3.0
$As_{30}Te_{70}$	0.5	2.47	0.030	2.4	2.66	0.065	2.9
$As_{20}Te_{80}$	0.2	2.48	0.010	2.8	2.65	0.074	3.0
Te K edge		Te-As			Te-Te		N_{Te}
Sample	N	r (Å)	σ (Å)	N	r (Å)	σ (Å)	
$As_{60}Te_{40}$	1.7	2.66	0.054	0.3	2.81	0.054	2.0
$As_{50}Te_{50}$	1.6	2.66	0.060	0.4	2.80	0.070	2.0
$As_{40}Te_{60}$	1.5	2.67	0.065	0.9	2.80	0.075	2.4
$As_{30}Te_{70}$	1.1	2.67	0.060	1.4	2.79	0.096	2.5

numbers, we use as an example the case of the $As_{40}Te_{60}$ glass. The correlations between the coordination numbers for the two different atomic pairs As-As and As-Te (or Te-Te and Te-As) are determined as follows: simulations of the filtered EXAFS spectrum at the As (or Te) edge are performed by fixing one coordination number, N_{AsAs} (or N_{TeTe}), and allowing all the other parameters to float. Figure 12 shows the factors of merit for such simulations, as well as the yielded N_{AsTe} (or N_{TeAs}). The minimum in the factor of merit allows us to determine the optimum set of parameters given in Table III and also to appreciate the uncertainty on their determinations, as given for values of the factors of merit twice larger than the minimum. As shown in Fig. 12(a), N_{AsAs} and N_{AsTe} appear to be rather strongly correlated. We would get $\Delta N_{AsTe} \sim \pm 0.25$ and $\Delta_{AsAs} \sim \pm 0.3$ from the values of the factors of merit twice larger than the minimum. However, as shown in Fig. 12(b), N_{TeAs} and N_{TeTe} are less correlated. Thus, from Fig. 12(b), the uncertainty for N_{TeTe} may be determined as ± 0.2 atom but only as ± 0.05 atom for N_{TeAs}. Through

$$N_{AsTe} = \frac{c_{Te}}{c_{As}} N_{TeAs} = 1.5 N_{TeAs} ,$$

we then have an uncertainty about ± 0.075 atom for N_{AsTe}. According to Fig. 12(a), such an error bar yields an uncertainty of ± 0.15 for N_{AsAs}. Similar analysis can be performed for all the samples. Finally the uncertainty for the partial coordination numbers is at most $\Delta N \sim \pm 0.2$, while error bars for interatomic distances are found to be within ± 0.01 Å. However, we point out that such an appreciation of the uncertainties may be an underestimation since it implicitly assumes a high quality for the phase shifts and amplitudes used in the fit.

As pointed out earlier, we may question the accuracy of the structural parameters determined from the EXAFS study. This is because on the one hand, the essential differences between the spectra, when passing from one composition to another situate in the low-energy range, where the theoretical formulation of the EXAFS process faces the difficulty due to the multiple-scattering process.

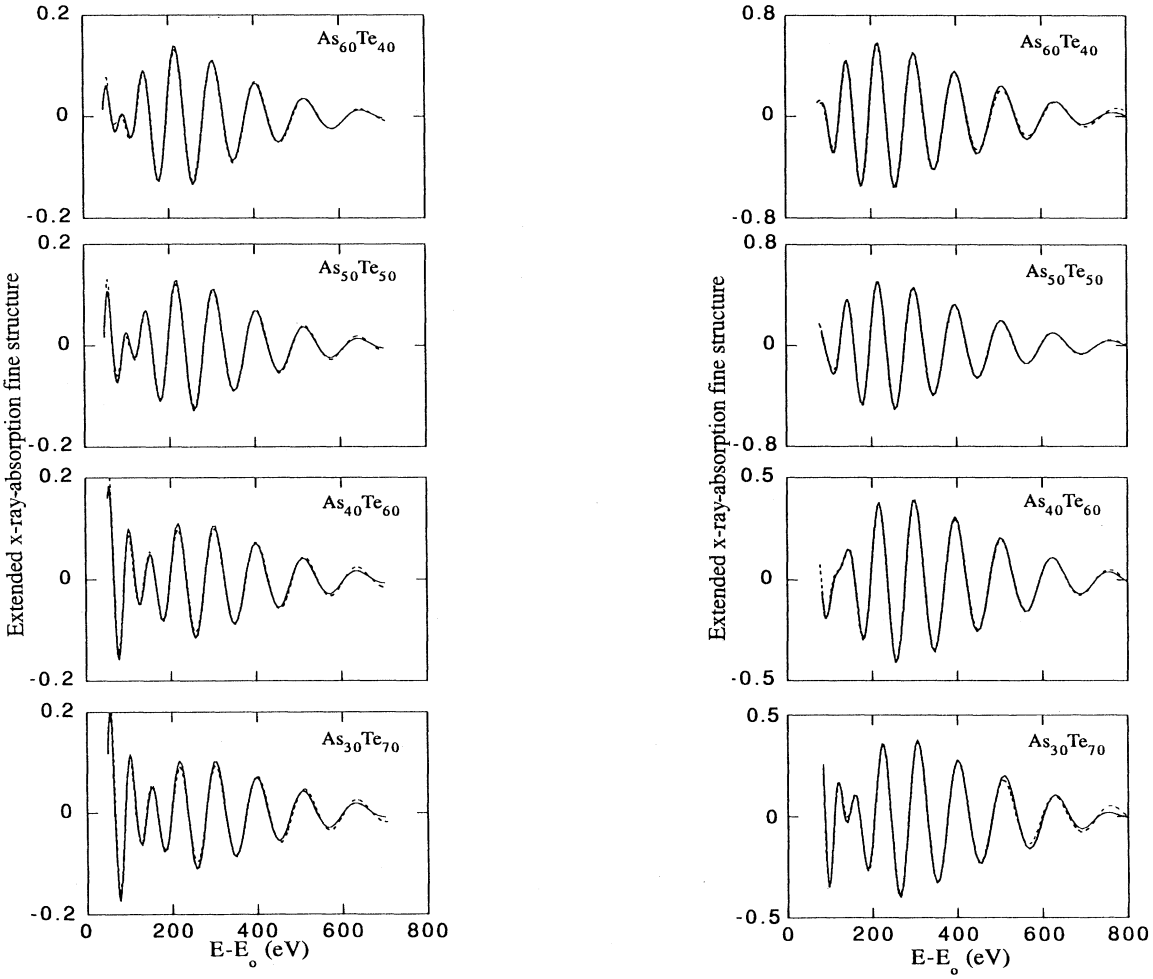

FIG. 11. Simulations of the glassy EXAFS spectra measured around the As (left) and Te (right) edges by using the calibrated Mac Kale *et al.* shifts and amplitudes. Fits are shown by dots and experimental data by full lines.

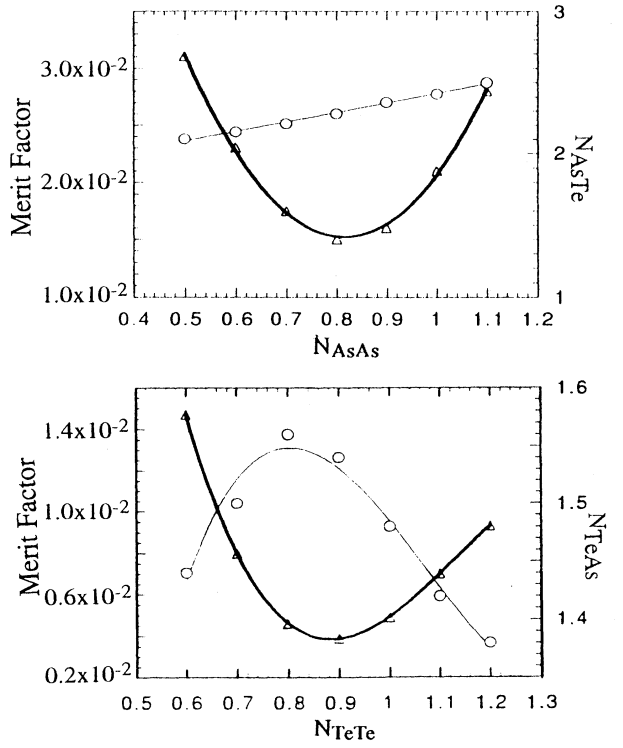

FIG. 12. Correlations between N_{AsAs} and N_{AsTe} (a) determined from the As K edge EXAFS and between N_{TeAs} and N_{TeTe} (b) determined from the Te K edge EXAFS (open circles). The corresponding values of the factor of merit are shown by open triangles.

On the other hand, the calibration of the Γ value for the As-Te or Te-As pair may be less accurate because of the weak EXAFS spectra of the crystalline $As_{40}Te_{60}$ β phase, so that it has been determined only over a short energy range. This may introduce systematic errors in the coordination number determinations. We thus now present the results of the DAS analysis for three glasses in order in verify these EXAFS results by using another technique.

IV. DIFFERENTIAL X-RAY ANOMALOUS SCATTERING RESULTS

The areas (N^*) and the interatomic distances (r) measured from the first peaks of the DDFs for the $As_{50}Te_{50}$ and $As_{40}Te_{60}$ glasses as well as for the RDF obtained at the As K edge for the $As_{20}Te_{80}$ glass are given in Table IV. The error bars were estimated by varying the parameters used in the data reduction, e.g., the density, the noise in the data, possible uncertainties in the values of the atomic scattering factors as well as the extension in k space over which the Fourier transformation from k to r space is performed.

TABLE IV. Interatomic distances and integrated areas of the first peaks of the DDFs.

Sample	$As_{50}Te_{50}$	$As_{40}Te_{60}$	$As_{20}Te_{80}$	Note
r (Å)	2.63±0.02	2.68±0.02		As-edge DDF
N^*	3.0±0.1	2.9±0.1		
r (Å)	2.75±0.02	2.75+00.02	2.76±0.02	Te-edge DDF
N^*	1.7±0.1	2.5±0.1	2.2±0.1	

The immediate important findings which can be derived from these results are (1) a drastic change in the Te coordination number occurring at the stoichiometric $As_{40}Te_{60}$ composition and (2) the mean interatomic distances, respectively, determined from the As- and Te-edge DDFs being significantly different, which readily indicate the existence of a chemical disorder in both the $As_{50}Te_{50}$ and $As_{40}Te_{60}$ glasses. The values N^* of the average coordination number around As atoms measured from the As DDFs also suggest the existence of chemical disorder in these glasses, because they are equal to 3 within the experimental uncertainty. Since we expect As atoms to be threefold coordinated, we can have an average coordination number of 3 only when assuming the simultaneous existence of As-As and As-Te pairs. The value $N^*=2.5$ measured from the Te DDF for the $As_{40}Te_{60}$ glass suggests that the Te coordination number should be larger than 2, since the calculation using the appropriate weights P_{ij} gives $N^*=1.6$ for two As neighbors and $N^*=2.25$ for two Te ones. This readily indicates the occurrence of threefold Te sites. These results are unambiguous since the distances and the N^* values given in Table IV are directly derived from the experimental measurements. They fully support our EXAFS results. Table V gives the P_{ij} values for different atomic pairs to show their contributions to the distribution functions. They are calculated by

$$P_{ij}=\frac{1}{c_i}W_{ij}(q=0)$$

when neglecting the q dependence of $W_{ij}(q)$.

To deconvolute the RDF or DDF, we assumed the Gaussian function $f_{ij}(r)$ as the shape of the contribution of each kind of atomic pairs to a given distribution peak. We then Fourier transform $N_{ij}f_{ij}(r)$ into q space and obtain $F_{ij}(q)$ as the model PSF. After multiplying $F_{ij}(q)$ by the corresponding $W_{ij}(q)$, we Fourier transform $F_{ij}(q)W_{ij}(q)$ back into r space using the same q range as that used to get the experimental RDF or DDF, and obtain the contribution of one kind of atomic pair to the given distribution peak. This procedure not only allows us to take into account the q dependence of $W_{ij}(q)$ but also to have similar broadening and truncation effects to those existing in the experimental RDF or DDF. The sum of the contributions calculated for different atomic pairs can be compared with the experimental data. We have checked that such a procedure yields coordination numbers within an uncertainty of 5%.

Obviously it is not possible to resolve the three contributions, i.e., from As-As, As-Te, and Te-Te, using only two DSFs. We thus started from the local structural model determined by the As-edge EXAFS data, which already gave a reasonable fit of the DDFs. We then adjusted various parameters to yield the best reconstruction. Note that the chemical compliance $c_{Te}N_{TeAs}=c_{As}N_{AsTe}$

TABLE V. Weights (P_{ij}) at $q=0$ for different atomic pairs in the distribution functions.

Sample	AsAs	AsTe	TeAs	TeTe	Note
$As_{50}Te_{50}$	0.68	1.30			As edge
			0.82	1.18	Te edge
$As_{40}Te_{60}$	0.63	1.23			As edge
			0.80	1.13	Te edge
$As_{20}Te_{80}$	0.06	0.25		1.00	RDF near the As edge

has been assumed in order to transfer N_{AsTe} to N_{TeAs} for the deconvolution of the Te-edge DDFs (and vice versa). In the case of the $As_{20}Te_{80}$ glass, we fixed N_{TeAs} at the value given by the EXAFS data and obtained N_{TeTe}. The structural parameters determined in this way are given in Table VI, together with the error bars within which the first distribution peaks can be well simulated. The agreement with the EXAFS results is reasonably good, which suggests the quality of the amplitudes and phase shifts used in our EXAFS analysis.

V. RELATIONS BETWEEN THE LOCAL ORDER AND SOME PHYSICAL PROPERTIES

Our results, clearly and consistently, show the following.

(i) As atoms are threefold coordinated throughout the compositional range. We have no evidence for sixfold coordinated As sites in Te-rich glasses, contrary to the assumption of Cornet and Rossier based on XPS data.[8]

(ii) Te atoms are twofold coordinated in As-rich alloys ($x>40$), while, the Te coordination suddenly increases to 2.4 at the stoichiometric $As_{40}Te_{60}$ composition, which indicates a large fraction (about 40%) of threefold Te sites in this glass. This percentage of occupancy seems to remain almost constant when further increasing the Te concentration.

(iii) A significant level of chemical disorder is evidenced by the existence of homopolar As-As and Te-Te bonds in the first coordination shell in all the investigated glasses. At the stoichiometric $As_{40}Te_{60}$ composition, the glassy structure is not chemically ordered and nearly the same amount of As-As and Te-Te bonds do exist in the first coordination shell. Thus it is very different from those of the $As_{40}S_{60}$ and $As_{40}Se_{60}$ glasses, which are chemically ordered.

(iv) The numbers of homopolar bonds monotonically evolve with composition.

(v) The local structures of glassy and crystalline $As_{40}Te_{60}$ are very different because of the chemical disorder and of the lower coordination numbers in the glassy state. Moreover, the weak EXAFS oscillations for the crystalline state are accounted for by a larger Debye-Waller factor, as shown in Table III, which indicates a larger dispersion of the interatomic distances in the first shell in the crystalline state. Obviously these results are at variance with those obtained by Cornet and Rossier[7] in quite a number of aspects.

We have no evidence, from small-angle x-ray scattering data, that glassy states are phase separated as discussed earlier. The fact that the values of the Debye-Waller factors for the As-As bonds in the glasses which range from 0 to 6×10^{-2} Å (see Table III) are smaller than that for amorphous elemental As ($\sim8.3\times10^{-2}$ Å) also seems to rule out the possibility of a phase separation in the glasses with the existence of arsenic amorphous clusters. Thus homopolar bonds should be *homogeneously* distributed in the glassy network. In order to understand the origin of the chemical disorder observed in the glasses, N_{AsAs} and N_{TeTe} (open squares) determined in this work are displayed, respectively, in Figs. 13(a) and 13(b) as a function of the arsenic concentration and compared with two extreme cases, i.e., the full chemical order (curve 1) and the full chemical disorder (curves 2 and 3), respectively, around As and Te atoms. In the calculation of the curve 1, we assumed $N_{AsAs}=0$ for $x\leq40$ and $N_{TeTe}=0$ for $x\geq40$. N_{AsAs} and N_{TeTe} in the case of chemical order are then calculated, respectively, for $N_{As}=3$ whatever the concentration and for $N_{Te}=2$ for $x>40$ while 2.5 for $x\leq40$ by using the relation $c_{As}N_{AsTe}=c_{Te}N_{TeAs}$. For a full chemical disorder around As, we have $N_{AsAs}=3c_{As}$, yielding the curve 2 in Fig. 13(a). By using the same relation, the curve 2 in Fig. 13(b) is obtained. The curve 3 describes a full chemical disorder around Te atoms, for which we have assumed $N_{TeTe}=2.5c_{Te}$ for $x\leq40$ and $N_{TeTe}=2c_{Te}$ for $x>40$. It is noted in Fig. 13(a) that for $x>40$, the atomic arrangement around As atoms shows a full chemical disorder, while for $x\leq40$, we find an intermediate situation between the two extreme cases. In Fig. 13(b), the atomic arrangement around Te atoms for

TABLE VI. Coordination numbers and interatomic distances from the DDF analysis. Coordination numbers determined from EXAFS are given in parentheses.

Sample	$As_{50}Te_{50}$		$As_{40}Te_{60}$		$As_{20}Te_{80}$	
pairs	N	r (Å)	N	r (Å)	N	r (Å)
As-As	1.5±0.1(1.6)	2.48±0.01	0.8±0.2(0.8)	2.47±0.01	(0.2)	
As-Te	1.5±0.1(1.4)	2.70±0.02	2.1±0.2(2.2)	2.69±0.02	(2.8)	
Te-As	1.5±0.1(1.6)	2.70±0.02	1.4±0.1(1.5)	2.69±0.02	0.7±0.1	2.67±0.01
Te-Te	0.4±0.1(0.4)	2.85±0.02	1.1±0.1(0.9)	2.83±0.02	1.7±0.1	2.80±0.01

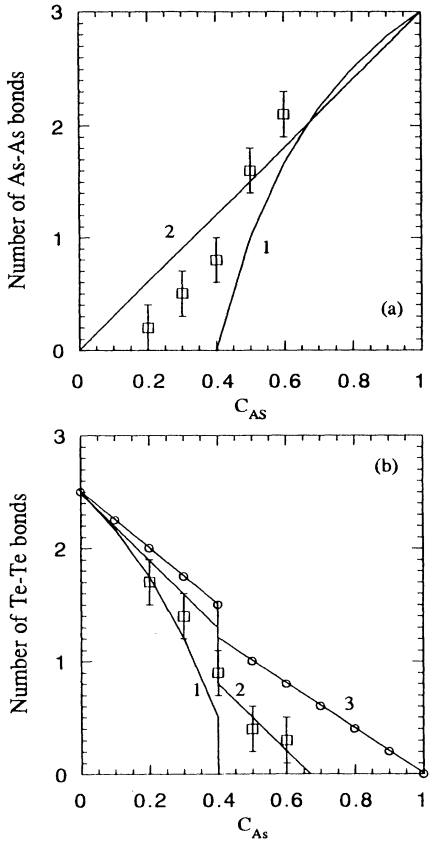

FIG. 13. The evolution of the chemical ordering with composition. Curve (1) is calculated for the full chemical order, while curves 2 and 3 for the full chemical disorder, respectively, around (a) As and (b) Te atoms. Open squares are the experimental values. Number of Te-Te bonds $=c_{TE}N_{TeTe}$ and number of As-As bond $=c_{As}N_{AsAs}$.

$x \leq 40$ also shows an intermediate situation, which is related to the one found in Fig. 13(a). However, the experimental data demonstrate a clear tendency towards the chemical order around Te atoms rather than towards the chemical disorder. For $x > 40$, the Te-Te bonds still exist probably until $x \sim 66$, as found by linearly extrapolating the N_{TeTe} curve towards that composition. This can be readily understood to be due to the full chemical disorder around As atoms since the experimental data agree well with the curve 2 for $x > 40$, as found in Fig. 13(b). These observations suggest that Te-Te bonds are less favored while As-As and As-Te are more favored, which is in good agreement with the bonding energy values reported in the literature,[32] which for the As-As, As-Te, and Te-Te bonds are 47.7, 45, and 38 kcal/mol, respectively. Since the bond energies for As-As and As-Te pairs are comparable, the atoms arrange themself around As just at random, resulting in the chemical disorder. But the significant difference in the energies for As-Te and Te-Te bonds makes As atoms more likely to bind to Te atoms, yielding the tendency towards the chemical order around Te atoms. The actual intermediate situation found for $x \leq 40$ is in fact due to the simultaneous requirements of the chemical order around Te atoms and of the chemical disorder around As atoms. Thus we have clarified the origin of the chemical disorder in the As_xTe_{100-x} glasses.

A. Glass forming ability (GFA) of As_xTe_{100-x} compounds

In recent years, the Phillips' constraint theory has often been applied to try to explain the physical properties of covalent glasses.[33,34] Phillips[33] suggested that a maximum of the GFA occurs when the number N_t of the constraints acting on one atom is equal to the number of the degrees of freedom, which is supposed to be equal to the space dimension N_d. The minimization of $(N_t - N_d)^2$ or of $\Delta = |N_d - N_t|$ is the condition to have a maximal GFA. In the three-dimensional space $N_d = 3$, each bond is associated to half the stretching constraint since it is shared by two atoms, and to $(2r-3)$ bending constraints. We thus have

$$\Delta = 3 - N_t = 3 - \sum_i c_i \left[\frac{r_i}{2} + (2r_i - 3) \right], \tag{5}$$

where r_i is the coordination number and c_i the atomic fraction for atoms of species i. The smaller the Δ value, the larger the GFA is. Setting $\Delta = 0$, we obtain an average coordination number $\langle m \rangle = 2.4$. In fact, the GFA can simply be evaluated by using $|\langle m \rangle - 2.4|$. As stated in the Introduction, the constraint theory broke down up to now in the case of As_xTe_{100-x} alloys. However, since our results are at large variance with the previous structural results, we may reexamine the GFA of these alloys using the constraint theory.

Figure 14 shows the variation of $\langle m \rangle$ (crosses) with composition. A prominent maximum can be observed at the stoichiometric composition. Following the Phillips' argument, the GFA for As_xTe_{100-x} compounds has to be minimal at this composition, which is consistent with the experimental observation. Instead of a well-constrained network as is the case for the $As_{40}S_{60}$ or $As_{40}Se_{60}$ glass, the glassy $As_{40}Te_{60}$ network is overconstrained due to the

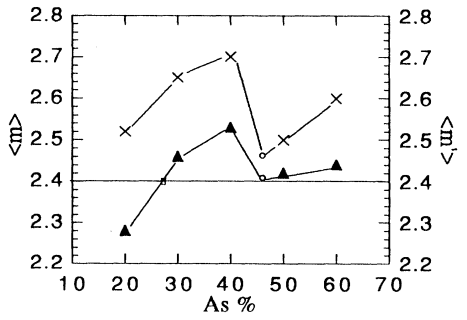

FIG. 14. Dependences of the mean coordination number on the composition: crosses represent the mean coordination numbers $\langle m \rangle$ and triangles the effective mean coordination numbers $\langle m' \rangle$ defined in text. Open square is obtained by interpolation and open circles by extrapolation. The error bar for $\langle m \rangle$ is ± 0.05.

increase in the mean coordination number around Te atoms at this composition. In addition, a drop in the $\langle m \rangle$ value appears around the $As_{50}Te_{50}$ composition. Extrapolating the $\langle m \rangle$ values obtained for the As-rich scale, we find that $\langle m \rangle$ reaches the critical value 2.4 at the $As_{46}Te_{54}$ eutectic as marked by an open circle, which has not, however, been experimentally investigated. This explains the easy obtention of the glassy state at this composition. On the Te-rich side, our results failed to explain the higher GFA at the $As_{27}Te_{73}$ eutectic at which a minimum of Δ does not appear. This may be due to the difficulty of correctly counting the constraint number. Such a difficulty occurs when the strengths of different bonds in the material are very different as already suggested by Thorpe for the silicate glasses.[34]

As stated, the Te-Te bond is significantly weaker than the As-As and As-Te ones. To try to take into account the bond strength, we give the Te-Te bonds a weaker weight (W) in the calculation of Δ in order to reduce their contribution to the glassy network and to recover a more correct constraint number. Since the GFA is maximum at the $As_{27}Te_{73}$ eutectic, we can calculate W for the Te-Te bonds to get an effective mean coordination number $\langle m' \rangle = 2.4$ for the glass at this composition, i.e.,

$$W = (2.4 - c_{As}N_{As} - c_{Te}N_{TeAS})/(c_{Te}N_{TeTe}) ,$$

where N_{TeAs} and N_{TeTe} are obtained by interpolation from the values experimentally determined for the $As_{20}Te_{80}$ and $As_{30}Te_{70}$ compositions. We thus get $W \sim 0.80$, which is used to calculate $\langle m' \rangle$, as shown by triangles in Fig. 14. Obviously, the interpretation of the compositional dependence of the GFA for As-rich glasses and for the $As_{40}Te_{60}$ glass still remains valid when using the $\langle m' \rangle$ values. $\langle m' \rangle$ for the $As_{20}Te_{80}$ glass is now smaller than 2.4, which explains the deterioration of the GFA on the Te-rich side of the $As_{27}Te_{73}$ composition. In this way the evolution of the GFA can be understood for all the compositions. This explanation is given here only to show the weakness of the constraint theory when it deals with a material in which a large difference among the bonding strengths exists and to suggest a possible explanation of the GFA behavior in the Te-rich domain. An appropriate treatment should differentiate the bond strengths.

B. Glass transition temperature T_g

Our structural results indicate a monotoneous change of the local chemical ordering with the composition. The T_g of As_xTe_{100-x} glasses also monotoneously evolves with composition. Such a compositional dependence of the T_g has been noted by several workers[5,35] and is also exhibited in our samples. Figure 15 illustrates a clear correlation between the number of strong As-As bonds, which is equal to the product of c_{As} and N_{AsAs}, and the T_g values for As_xTe_{100-x} glasses, which were reported by Cornet and Rossier.[5] It appears that the glassy structure is stabilized with the increase of the number of As-As bonds. This supports the argument that the T_g is mainly determined by the stronger bonding forces in the glassy

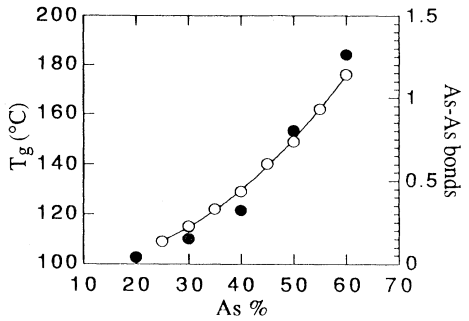

FIG. 15. Compositional dependences of T_g (open circles) and of the number of the As-As bonds (black circles).

structure.[36] Based on this argument, we may also understand why the T_g values of As_xS_{100-x} or As_xSe_{100-x} glasses show a maximum at the stoichiometric composition. Structural studies[37,38] have shown that the chemical ordering is obeyed in these glasses, so that there are no homopolar bonds appearing in the glass at the $As_{40}X_{60}$ (X=S or Se) composition. Among three kinds of atomic bond, the heteropolar bonds, i.e., As-S or As-Se, should be the most favored and thus the most stable. Since the number of the heteropolar bonds reaches the maximum at the $As_{40}X_{60}$ (X=S or Se) composition, yielding a stable glassy network, the maximum T_g value is thus observed for the glass with this composition.

C. Microhardness

Figure 16 shows the compositional dependence of the microhardness K (solid triangles), which were measured by Cornet and Rossier,[5] and of the number of As-As bonds. They coincide with each other. In comparison with the T_g, the microhardness shows an even clearer correlation with the number of strong As-As bonds. This is in accordance with the argument that the microhardness is sensitive to the local order. We thus suggest that it is mainly related to the strong As-As bonds and not simply to the average coordination number $\langle m \rangle$. Noticing the sudden drop of $\langle m \rangle$ when passing from $As_{40}Te_{60}$

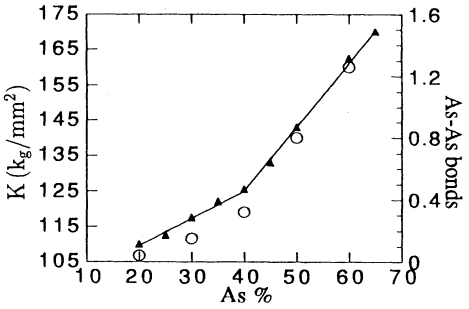

FIG. 16. Compositional dependences of the microhardness (solid triangles) and of the number of the As-As bonds (open circles).

(~ 2.7) to $As_{50}Te_{50}$ (~ 2.5), we find that Thorpe's concepts of "rigidity" for overstrained networks with $\langle m \rangle > 2.4$ and "floppiness" for underconstrained ones with $\langle m \rangle < 2.4$ do not apply to As_xTe_{100-x} glasses: for instance, $\langle m \rangle$ is smaller for the $As_{50}Te_{50}$ glass than for the $As_{40}Te_{60}$ one, thus the first should be more rigid than the latter though experimentally the situation is reversed as the K curve shows. The reason for the failure is not completely clear, but we think that it is probably also due to the fact that the constraint theory treats different bonding forces on the same level. In our opinion, the strong bonds dominate the mechanical properties.

D. Electronic conductivity

Figure 17 compares the compositional dependences of the conductivity $\sigma_{20°C}$ (open circles) for As_xTe_{100-x} glasses, the data being taken from Ref. 2 and of the number of Te-Te bonds. It thus appears that σ is related to the number of Te-Te bonds and thus to the local order, which is believed to primarily determine the electric conductivity. Elliott[39] pointed out that the width of the band gap of a material is governed, to a large extent, by the strength of the bonds which are present. Our results support this argument. The increase of the number of the weak Te-Te bonds and the decrease of that of the strong As-As and As-Te ones with increasing the Te concentration cause the shrinkage of the band gap and thus the increase of σ.

The correlation shown in Fig. 17 explains the main tendency of the evolution of σ with the composition. We would like, however, to suggest a simply physical mechanism, which may explain the relatively steep increase of the σ values for Te-rich glasses ($x \leq 40$). It occurs at the $As_{40}Te_{60}$ composition, at which a large amount of threefold Te sites appears in the glassy structure. Since a chalcogen atom has four electrons in its outer p orbitals, a twofold coordinated Te atom has a lone pair band whose energy is higher than that of the valence band. But a threefold coordinated Te atom has three p electrons involved in the bonding with the neighboring atoms, forming the filled valance band. There is only one electron left which is unstable. This electron may either be promoted into the conducting band or be trapped in a defect site. If we assume that this electron lies in the conducting band and takes part in the conduction, the threefold Te atom now bears metallic character in the sense of the transport property. In this case, the appearance of threefold Te atoms is the main origin of the steep increase of σ starting out at $As_{40}Te_{60}$.

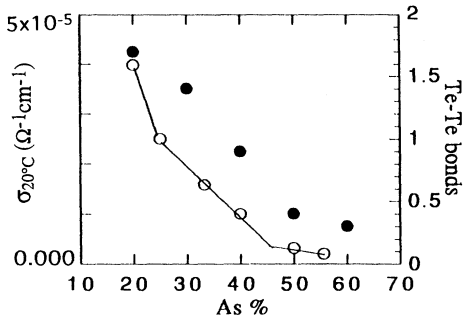

FIG. 17. Compositional dependences of the conductivity (open circles) and of the number of the Te-Te bonds (solid circles).

The other possibility that the single electron is trapped in a defect site on a chalcogen atom has been proposed by Street and Mott[40] in order to explain the absence of electron spin resonance (ESR) signals in chalcogenide glasses. Since it accommodates the transferred electron, this chalcogen atom then becomes onefold coordinated and has two lone pairs. Thus, there should exist in the glass threefold positively charged as well as onefold negatively charged sites, in addition to twofold neutral ones. In our opinion, it is unlikely that the Mott's mechanism applies to the As_xTe_{100-x} glasses. The decisive reason is that it requires the same amount of onefold Te sites and of threefold Te sites to accommodate the transferred electrons. If this were the case, the mean coordination number around Te for Te-rich glasses should be much smaller than 2.5, and indeed equal to 2. This is inconsistent with the structural results obtained in this work.

VI. CONCLUSIONS

By using EXAFS and difference anomalous scattering which both allow us to selectively probe the environment around each component, we have determined the local ordering in As_xTe_{100-x} glasses. We have found the chemical disorder in these glasses. To our opinion, the bonding strength plays a dominant role in the arrangement of chemically different constitutes in the solid state. The chemical disorder in As_xTe_{100-x} glasses should directly result from the fact that the As-As and As-Te bonds have similar bonding forces, while the chemical ordering is dominated by the strongest As-S or As-Se bonds in As_xS_{100-x} or As_xSe_{100-x} glasses. We have also observed a sudden increase of the Te coordination from 2 to 2.4 at the $As_{40}Te_{60}$ composition, which indicates that an amount of Te atoms undertakes a valence change at the stoichiometric composition. The observation of the chemical disorder as well as the valence change of the Te atom at the $As_{40}Te_{60}$ composition demonstrate that the $As_{40}Te_{60}$ glass is very different from the $As_{40}Se_{60}$ and $As_{40}S_{60}$ glasses. Based on our structural results, we have suggested possible explanations for some peculiar features of the macroscopic properties of these glasses, such as the GFA, the T_g, the microhardness and the conductivity, which are related either to the monotonic evolution of the chemical ordering with composition or the valence change of the Te atom at the $As_{40}Te_{60}$ composition.

ACKNOWLEDGMENTS

We would like to thank Dr. Peter Kizler from Hasylab for his efficient assistance for the Te*K* edge EXAFS measurements. Our thanks also go to R. Ollitrault at the Université Paris V and to A. Dezellus at CECM for their guidance to the sample preparation. We acknowledge stimulating discussions with J. P. Gaspard and we thank M. Ribes for the electron microscopy experiments and O. Lyon for x-ray small-angle scattering measurements.

[1]S. R. Elliott, *Physics of Amorphous Materials* (Longman Scientific & Technical and Wiley, New York, 1990).
[2]Z. U. Borisova, *Glassy Semiconductors* (Plenum, New York, 1981).
[3]J. A. Savage, in *Glass. . . Current Issues,* edited by A. F. Wright and J. Dupuy (Martinus Nijhoff, Netherlands, 1985).
[4]S. R. Ovshinsky, Phys. Rev. Lett. **21**, 1450 (1968).
[5]J. Cornet and D. Rossier, J. Non-Cryst. Solids **12**, 62 (1973).
[6]J. R. Fitzpatrick and C. Maghrab, Phys. Chem. Glasses **12**, 105 (1971).
[7]J. Cornet and D. Rossier, J. Non-Cryst. Solids **12**, 84 (1973).
[8]J. Cornet and D. Rossier, in *The Structure of Non Crystalline Materials,* edited by Ph. Gaskell (Taylor and Francis, London, 1977), p. 17.
[9]M. Tenhover, P. Boolchand, and W. J. Bresser, Phys. Rev. B **27**, 7533 (1983).
[10]R. F. Pettifer, Ph.D. thesis, Dept. of Physics, University of Warwick, 1978.
[11]J. C. Phillips, J. Non-Cryst. Solids **34**, 153 (1979).
[12]S. Tsugane, M. Haradome, and R. Hioki, Jpn. J. Appl. Phys. **4**, 77 (1977).
[13]J. Cornet and D. Rossier, Mater. Res. Bull **8**, 9 (1973).
[14]R. Quinn, Mater. Res. Bull. **9**, 803 (1974).
[15]M. Tenhover, P. Boolchand, and W. J. Bresser, Bull. Am. Phys. Soc. **27**, 1509 (1983).
[16]J. A. Savage, J. Non-Cryst. Solids **11**, 122 (1972).
[17]J. C. Rouland, R. Ollitrault-Richet, J. Flahaut, J. Rivert, and R. Ceolin, Thermochim. Acta **161**, 189 (1990).
[18]Uwe Köster, in *Glass. . . Current Issues* (Ref. 3).
[19]M. Ribes (private communication).
[20]Haw Wan Shu, S. Jaulmes, and J. Flahaut, Mater. Res. Bull. **21**, 1509 (1986).
[21]G. N. Greaves, S. R. Elliott, and E. A. Davis, Adv. Phys. **28**, 49 (1979).
[22]R. W. G. Wyckoff, *Crystal Structures,* 2nd ed. (Interscience, New York, 1965), Vol. 1, p. 36.
[23]E. A. Stern, Phys. Rev. B **10**, 3027 (1974).
[24]A. G. Mac Kale, B. W. Vael, A. P. Paulikas, S. K. Chan, and G. S. Knapp, J. Am. Chem. Soc. **110**, 3763 (1988).
[25]P. H. Fuoss, P. Eisenberger, W. K. Warburton, and A. Bienenstock, Phys. Rev. Lett. **46**, 1537 (1981).
[26]D. T. Cromer and J. B. Mann, Acta. Cryst. A **21**, 321 (1968).
[27]Sasaki, KEK Report 83-22, National Laboratory for High Energy Physics, Tsukuba, Japan, 1983 (unpublished).
[28]R. W. James, *The Optical Principles of the Diffraction of X-rays* (Bell, London, 1983).
[29]G. Palinkas, Acta Cryst. A **29**, 10 (1973).
[30]J. Krogh, Acta Cryst. **9**, 951 (1956); N. Norman, *ibid.* **19**, 370 (1957).
[31]P. Armand, A. Ibanez, E. Philippot, Q. Ma, and D. Raoux, J. Non-Cryst. Solids **150**, 371 (1992).
[32]K. Nandakumar and J. Philip, J. Non-Cryst. Solids **144**, 247 (1992).
[33]J. C. Phillips, J. Non-Cryst. Solids **34**, 153 (1981); **43**, 37 (1979).
[34]M. F. Thorpe, J. Non-Cryst. Solids **57**, 355 (1983).
[35]R. K. Quinn, Mater. Res. Bull. **9**, 803 (1974).
[36]P. R. Couchman, Solid State Commun. **77**, 553 (1991).
[37]C. Y. Yang, M. A. Paesler, and D. E. Sayers, Phys. Rev. B **39**, 10 342 (1989).
[38]V. R. Mastelaro, S. Benazeth, and H. Dexpert, J. Solid State Chem. **96**, 301 (1992).
[39]S. R. Elliott, in *Glass. . . Current Issues* (Ref. 3), p. 395.
[40]R. A. Street and N. F. Mott, Phys. Rev. Lett. **35**, 1293 (1975).